Electronic Supplementary Material (ESI) for Soft Matter.

MPTTF-Containing Tripeptide-Based Organogels: Receptor for 2, 4, 6-Trinitrophenol and Multiple Stimuli-Responsive Properties

Yucun Liu, Yuan Wang, Longyi Jin, Tie Chen* and Bingzhu Yin*

Key Laboratory of Natural Resources of Changbai Mountain & Functional Molecules of Ministry of Education, Yanbian University, Yanji, Jilin 133002, PR China.

E-mail: zqcong@ybu.edu.cn;

Fax: +86 433 2732456;

Tel: +86 433 2732298.

1. Instrumentation

Gelation study

A weight amount of the gelator **1** with or without TNP adding a measured volume of the solvent were placed in a sealed test tube and made a clear solution by heating. And then, the system left at room temperature. The transition temperatures (T_{gel}) were determined by ball-drop method.

NMR experiments

All solution state NMR studies were carried out on Bruker AV-300 Spectrometer (300 MHz for ^{1}H and 75 MHz for ^{13}C) and chemical shifts were referenced relative to tetramethylsilane (δ_H/δ_C=0).

FT-IR spectroscopy

IR spectra were recorded on a Shimadzu FT-IR Prestige-21 instrument with the KBr disk technique.

MALDI-TOF-MS spectrometry

Mass spectra were performed on a Shimadzu Axima CFR^{TM} Plus using a 1,8,9-anthracenetriol (DITH) and β-phenylacrylic acid (CHCA) matrix.

Cyclic voltammetry

Cyclic voltammetry was performed with CHI660D instruments in a mixture of CH_2Cl_2 / CH_3CN (v:v = 1:1) with 0.1 M Bu_4NPF_6 as the supporting electrolyte and a scan rate of 100 mVs^{-1}. Counter and working electrodes were made of Pt and glass carbon, respectively, and an Ag/AgCl was used as the reference electrode. A small amount of the gel or CT gel was carefully put on the glass carbon electrode, which was left in air for 24h.

UV-vis spectroscopy

UV-vis spectra were recorded on a Hitachi U-3010 spectrophotometer.

Circular dichroism (CD) spectroscopy

CD spectra were obtained on Chirascan spectrometer using a 1 mm path-length cell.

Atomic force microscopy (AFM)

For AFM experiments, 10 μL of sample solution (diluted gels) was drop-casted onto a freshly cleaved mica surface. Each sample was air-dried 48 h in a dust-free environment prior to AFM imaging. The images were obtained by scanning the mica surfaces in air under ambient conditions

using Agilent-5500 in tapping mode.

Field emission scanning electron microscopy

The gel samples were placed on silicon wafer, and dried for 24 h under room temperature before imaging. A layer of gold was sputtered on top to form a conducting surface and finally the specimen was transferred into the Field Emission Scanning Electron Microscope (FE-SEM, Joel Scanning Microscope-JSM-6700F).

Small-angle X-ray diffracting

Small-angle X-ray scattering (SAXS) measurements were carried out at 298 K on a beamline 1W2A synchrotron radiation X-ray small angle system at Beijing Synchrotron Radiation Facility(λ =1.54Å).

Wide-angle x-ray diffraction

Wide-angle X-ray diffracting (WAXRD) measurements were carried out at 298 K on the glass-sustained xerogel films and recorded on a Bruker D8/ADVANCE X-ray diffractmeter (Germany) with radiation (λ =1.54Å) at Chang Chun Institute of Applied Chemistry Chinese Academy of Sciences.

2. Synthetic procedure and Characterization

All the amino and carboxyl coupling reactions were carried out using the standard EDCI/HOBt method.[1] Firstly, tert-butyloxycarbonyl (Boc)-protected L-amino acids was coupled with the methyl ester protected L-amino acids by using EDCI (1.2 equiv.) and HOBt (1.2 equiv.) in dry dichloromethane. After reaction finishing, the coupled product was washed sequentially with water, dilute NaOH and water to neutrality. The crude product was purified by flash chromatography (SiO_2, 100-200mesh). The product was subjected to hydrolysis with 1 M NaOH solution in methanol followed by workup with 1 M HCl. Adding in the ethyl acetate and the organic part was dried over anhydrous sodium sulphate and the solvent was evaporated to get the crude coupled product. The free acid terminus of the L-dipeptide was further coupled with *n*-dodecylamine by using EDCI/HOBt, similarly to the procedure described above. Then, the corresponding N-Boc-protected of the product was subjected to deprotection by TFA (20 equiv.) in dry DCM. After stirring for 2 h, solvents were removed on a rotary evaporator. The residue obtained was repeatedly dissolved in dichloromethane and the solvent evaporated to yield the crude trifluoroacetate salt, which was taken in ethyl acetate. The EtOAc part was thoroughly washed with saturated sodium bicarbonate solution and brine to neutrality. The organic part was dried over anhydrous sodium sulphate and concentrated to get the corresponding amine which was used in the next step without further purification. Following a similar method, monochloroacetic acid was coupled with the corresponding amines by using EDCI/HOBt in dry dichloromethane stirring at room temperature for 1 d. Collecting the generated white solids and recrystallization from methanol to afford the corresponding intermediate products. Finally, the got intermediate compounds were reacted with MPTTF [2] by using Cs_2CO_3 as a base in dry THF/CH_3CN. The resultant reaction mixture was then filtered and the filtrate was concentrated in a rotary evaporator. The crude products were purified by flash chromatography (SiO_2, 100-200mesh) with MeOH/CH_2Cl_2 as the eluents, respectively.

Reference:

1. a) S. Debnath, A. Shome, S. Dutta and P. K. Das, *Chem. Eur. J.*, 2008, 14, 6870-6881; b) P. Fatás, J. Bachl, S. Oehm, A. I. Jiménez, C. Cativiela and D. Díaz Díaz, *Chem. Eur. J.*, 2013, **19**, 8861-8874; c) D. K. and A.Banerjee, *Chem. Asian J.*, 2012, **8**, 113-120; d) D. Mandal, T. Kar, and P. K. Das, *Chem. Eur. J.*, 2013, **19**, 1349-1358; e) B. Adhikari, C. Singh, A. Shah, A. J. Lough and H. Kraatz, *Chem. Eur. J.*, 2015, **21**, 11560-11572.

2. a) J. O. Jeppesen, K. Takimiya, F. Jensen, T. Brimert, K. Nielsen, N. Thorup and J. Becher, *J. Org. Chem.*, 2000, **65**, 5794-5805; b) M. Takase, N. Yoshida, T. Nishinaga and M. Iyoda, *Org. Lett.*, 2011, **13**, 3896-3899. c) Y. Liu, N. Zheng, H. Li and B. Yin, *Soft Matter*, 2013, **9**, 5261-5269.

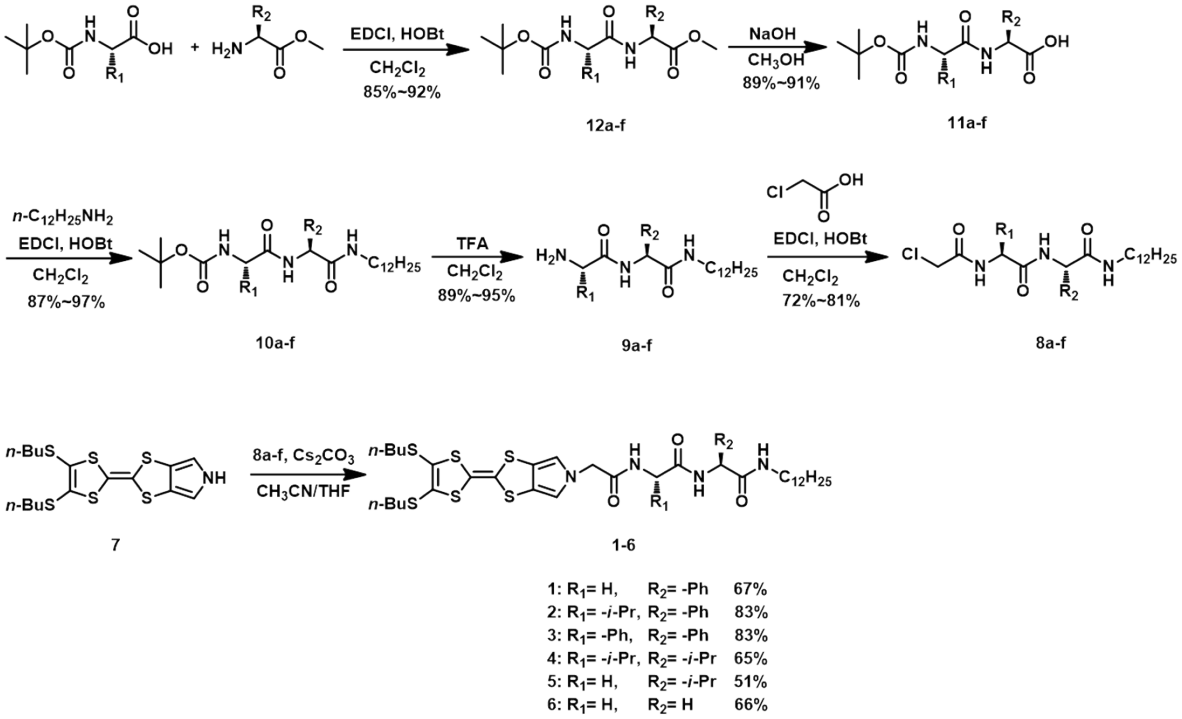

Characterization of intermediate compounds 10

Characterization of 10a (BOC-Gly-Phe-NH-$C_{12}H_{25}$)

White solid. m.p. 108-109°C; ^{1}H NMR (300 MHz, $CDCl_3$) δ 0.88 (t, J = 6 Hz, 3H), 1.15-1.37 (m, 27 H), 1.73 (br, 2H), 3.02-3.08 (m, 2H), 3.10-3.23 (m, 2H), 3.32 (s, 2H), 4.58 (q, J = 9 Hz, 1H), 5.98 (t, J = 4.5 Hz, 1H), 7.21-7.31 (m, 5H), 7.82 (d, J = 9 Hz, 1H); ^{13}C NMR (75 MHz, $CDCl_3$) δ 172.70, 170.58, 159.70, 137.02, 129.29, 128.65, 126.96, 79.84, 54.57, 44.53, 39.58, 38.46, 31.98, 29.71, 29.66, 29.58, 29.42, 29.34, 29.31, 29.26, 26.86, 22.76, 14.19; MALDI-TOF MS m/z Calcd for $C_{28}H_{47}N_3O_4$: 489.36. Found: 390.4 ([M-Boc+2H]$^+$, 100).

Characterization of 10b (BOC-Leu-Phe-NH-$C_{12}H_{25}$)

White solid. m.p. 155-156°C; ^{1}H NMR (300 MHz, $CDCl_3$) δ 0.88 (t, J = 6 Hz, 3H), 1.22-1.36 (m, 36H), 1.50-1.56 (m, 2H), 3.08-3.18 (m, 3H), 3.26-3.34 (m, 2H), 4.52 (q, J = 9 Hz, 1H), 5.63 (t, J = 4.5 Hz, 1H), 7.21-7.33 (m, 5H), 7.40 (t, J = 5.7 Hz, 1H), 8.06 (d, J = 8.4 Hz, 1H); ^{13}C NMR (75 MHz, $CDCl_3$) δ 169.19, 159.80, 158.93, 136.19, 129.23, 128.71, 127.10, 80.55, 55.24, 39.75, 39.59, 38.20, 31.86, 29.57, 29.44, 29.29, 29.16, 26.79, 26.70, 22.63, 14.06; MALDI-TOF MS m/z Calcd for $C_{32}H_{55}N_3O_4$: 449.42. Found: 450.3 ([M+1]$^+$, 100).

Characterization of 10c (BOC-Phe-Phe-NH-$C_{12}H_{25}$)

White solid. m.p. 165-156°C; ^{1}H NMR (300 MHz, $CDCl_3$) δ 0.88 (t, J = 6 Hz, 3H), 1.22-1.36 (m,

27H), 1.50-1.58 (m, 2H), 3.09-3.17 (m, 2H), 3.29 (q, J = 6 Hz, 4H), 4.52 (q, J = 6 Hz, 2H), 5.62 (t, J = 5.4 Hz, 1H), 7.21-7.33 (m, 10H), 7.40 (t, J = 6 Hz, 1H), 8.05 (d, J = 8.7 Hz, 1H); ^{13}C NMR (75 MHz, $CDCl_3$) δ169.29, 159.91, 159.04, 136.30, 129.34, 128.83, 127.22, 79.58, 55.36, 39.86, 39.70, 38.31, 31.97, 29.69, 29.68, 29.64, 29.56, 29.40, 29.27, 26.90, 26.82, 22.74, 14.17; MALDI-TOF MS m/z Calcd for $C_{35}H_{53}N_3O_4$: 571.41. Found: 571.7 ($[M]^+$, 100).

Characterization of 10d (BOC-Leu-Leu-NH-$C_{12}H_{25}$)

Colourless oil liquid. ^{1}H NMR (300 MHz, $CDCl_3$) δ 0.86-0.93 (m, 15H), 1.25-1.37 (m, 20H), 1.44 (s, 9H), 1.55-1.66 (m, 6H), 3.12-3.29 (m, 2H), 4.18 (br, 1H), 4.49 (br, 1H), 5.42 (br, 1H), 6.97 (t, J = 6 Hz, 1H), 7.13 (t, J = 6 Hz, 1H); ^{13}C NMR (75 MHz, $CDCl_3$) δ172.87, 171.83, 155.82, 79.98, 53.28, 51.81, 41.30, 40.99, 39.59, 31.93, 29.68, 29.66, 29.60, 29.49, 29.37, 28.34, 26.97, 24.76, 22.94, 22.70, 22.15, 14.13; MALDI-TOF MS m/z Calcd for $C_{29}H_{57}N_3O_4$: 511.43. Found: 511.8 ($[M]^+$, 100).

Characterization of 10e (BOC-Gly-Leu-NH-$C_{12}H_{25}$)

White solid. m.p. 121-122^{o}C; ^{1}H NMR (300 MHz, $CDCl_3$) δ 0.86-0.94 (m, 9H), 1.25-1.37 (m, 19H), 1.45-1.51 (m, 11H), 1.58-1.66 (m, 2H), 3.12-3.31 (m, 2H), 3.80 (s, 2H), 4.43 (q, J = 8.4 Hz, 1H), 5.34 (br, 1H), 6.54 (t, J = 8.7 Hz, 1H), 6.81 (t, J = 8.4 Hz, 1H); ^{13}C NMR (75 MHz, $CDCl_3$) δ168.21, 166.19, 155.71, 76.95, 48.37, 40.96, 37.72, 36.28, 28.51, 26.25, 26.20, 26.14, 26.00, 25.95, 25.88, 24.87, 23.50, 21.35, 19.49, 19.28, 18.68, 10.71; MALDI-TOF MS m/z Calcd for $C_{25}H_{49}N_3O_4$: 455.37. Found: 399.7 ($[M\text{-isobutyl}+2H]^+$, 100).

Characterization of 10f (BOC-Gly-Gly-NH-$C_{12}H_{25}$)

White solid. m.p. 78-79^{o}C; ^{1}H NMR (300 MHz, $CDCl_3$) δ 0.89 (t, J = 6 Hz, 3H), 1.24-1.35 (m, 18H), 1.46-1.53 (s, 11H), 3.24 (q, J = 6.6 Hz, 2H), 3.83 (d, J = 3.9 Hz, 2H), 3.95 (d, J = 5.1 Hz, 2H), 5.43 (br, 1H), 6.60 (br, 1H), 7.12 (br, 1H); ^{13}C NMR (75 MHz, $CDCl_3$) δ170.05, 168.65, 156.41, 80.48, 44.53, 43.15, 39.80, 31.95, 29.69, 29.58, 29.46, 29.38, 29.34, 28.35, 26.95, 22.72, 14.15; MALDI-TOF MS m/z Calcd for $C_{21}H_{41}N_3O_4$: 399.31. Found: 398.6 ($[M\text{-}1]^+$, 100).

Cleavage of the N-Boc protecting group and get compounds 9

Trifluoroacetic acid (TFA, 10 mL) was added to a solution of the corresponding N-Boc-protected compound (ca. 2 g) in dichloromethane (15 mL). The solution was stirred at room temperature for 2 h and evaporated. The residue obtained was repeatedly dissolved in dichloromethane and the solvent evaporated to yield the crude trifluoroacetate salt, which was redissolved in

dichloromethane (60 mL) and washed with saturated aqueous $NaHCO_3$ (3 x 40 mL) and brine to neutrality. After drying and filtering, evaporation of the solvent afforded the corresponding amine which was used in the next step without further purification.

Characterization of intermediate compounds 8

Characterization of 8a (Chloracetyl-Gly-Phe-NH-$C_{12}H_{25}$)

White solid. m.p. 128-129°C; ^{1}H NMR (300 MHz, d_6-DMSO) δ 0.85 (t, J = 6 Hz, 3H), 1.24-1.40 (m, 20H), 2.73-3.11 (m, 4H), 3.6-3.82 (m, 2H), 4.11 (s, 2H), 4.41-4.49 (m, 1H), 7.16-7.27 (m, 5H), 7.92 (t, J = 5.1 Hz, 1H), 8.21 (d, J = 8.4 Hz, 1H), 8.35 (t, J = 5.4 Hz, 1H); ^{13}C NMR (75 MHz, d_6-DMSO) δ 170.28, 167.84, 166.22, 137.67, 129.10, 127.86, 126.22, 54.08, 42.43, 42.14, 38.51, 37.95, 31.29, 29.05, 29.01, 28.96, 28.89, 28.71, 26.28, 22.08, 13.93; MALDI-TOF MS m/z Calcd for $C_{25}H_{40}ClN_3O_3$: 465.28. Found: 389.5 ([M-chloracetyl+2H]$^+$, 100).

Characterization of 8b (Chloracetyl-Leu-Phe-NH-$C_{12}H_{25}$)

White solid. m.p. 162-163°C; ^{1}H NMR (300 MHz, d_6-DMSO) δ 0.70-0.86 (m, 9H), 1.24-1.54 (m, 23H), 2.71-3.08 (m, 4H), 4.08 (s, 2H), 4.26-4.39 (m, 1H), 4.42-4.46 (m, 1H), 7.12-7.22 (m, 5H), 7.77 (t, J = 5.1 Hz, 1H), 8.12 (d, J = 7.2 Hz, 1H), 8.28 (t, J = 6.3 Hz, 1H); ^{13}C NMR (75 MHz, d_6-DMSO) δ 171.14, 170.27, 165.72, 137.70, 129.11, 127.97, 126.18, 53.94, 51.41, 42.54, 40.88, 38.43, 37.65, 31.28, 29.05, 29.00, 28.87, 28.74, 28.70, 26.22, 24.06, 22.92, 22.54, 22.08, 21.66, 13.93; MALDI-TOF MS m/z Calcd for $C_{29}H_{48}ClN_3O_3$:521.34. Found: 521.3 ([M]$^+$, 100).

Characterization of 8c (Chloracetyl-Phe-Phe-NH-$C_{12}H_{25}$)

White solid. m.p. 167-168°C; ^{1}H NMR (300 MHz, d_6-DMSO) δ 0.85 (t, J = 6.3 Hz, 3H), 1.23-1.41 (m, 20H), 2.65-3.10 (m, 6H), 4.00 (s, 2H), 4.42-4.59 (m, 2H), 7.15-7.27 (m, 10H), 7.81 (t, J = 5.4 Hz, 1H), 8.25-8.33 (m, 2H); ^{13}C NMR (75 MHz, d_6-DMSO) δ 170.24, 170.18, 165.48, 137.63, 137.31, 129.23, 129.16, 128.02, 127.88, 126.25, 54.12, 53.91, 42.42, 38.47, 37.54, 31.30, 29.07, 29.02, 28.92, 28.77, 28.72, 26.27, 22.09, 13.95; MALDI-TOF MS m/z Calcd for $C_{32}H_{46}ClN_3O_3$: 555.32. Found: 555.2 ([M]$^+$, 100).

Characterization of 8d (Chloracetyl-Leu-Leu-NH-$C_{12}H_{25}$)

White solid. m.p. 157-158°C; ^{1}H NMR (300 MHz, d_6-DMSO) δ 0.82-0.89 (m, 15H), 1.24 (br, 18H), 1.36 (t, J = 6 Hz, 2H), 1.41-1.46 (m, 4H), 1.51-1.62 (m, 2H), 2.93-3.10 (m, 2H), 4.10 (s, 2H), 4.24 (q, J = 8.4 Hz, 1H), 4.33 (q, J = 7.5 Hz, 1H), 7.75 (t, J = 8.4 Hz, 1H), 8.02 (d, J = 8.1 Hz, 1H), 8.31 (d, J = 8.1 Hz, 1H); ^{13}C NMR (75 MHz, d_6-DMSO) δ 171.38, 171.15, 165.74, 51.35, 51.10, 42.54, 40.98, 40.90, 38.32, 31.28, 29.04, 28.99, 28.92, 28.70, 26.20, 24.18, 24.12, 22.98,

22.84, 22.07, 21.76, 21.64, 13.92; MALDI-TOF MS m/z Calcd for $C_{26}H_{50}ClN_3O_3$: 487.35. Found: 488.6 ($[M+1]^+$, 100).

Characterization of 8e (Chloracetyl-Gly-Leu-NH-$C_{12}H_{25}$)

White solid. m.p. 140-141°C; ^{1}H NMR (300 MHz, d_6-DMSO) δ 0.82-0.89 (m, 9H), 1.24 (br, 18H), 1.36-1.45 (m, 3H), 1.48-1.60 (m, 2H), 2.91-3.11 (m, 2H), 3.76-3.79 (m, 2H), 4.13 (s, 2H), 4.25 (q, J = 8.1 Hz, 1H), 7.88 (t, J = 5.4 Hz, 1H), 8.05 (d, J = 8.4 Hz, 1H), 8.39 (t, J = 5.4 Hz, 1H); ^{13}C NMR (75 MHz, d_6-DMSO) δ 171.46, 167.89, 166.10, 51.03, 42.47, 42.22, 41.17, 38.44, 31.27, 29.02, 28.98, 28.68, 26.26, 24.18, 24.16, 22.94, 22.89, 22.08, 22.06, 21.69, 21.67, 13.93; MALDI-TOF MS m/z Calcd for $C_{22}H_{42}ClN_3O_3$: 431.29. Found: 432.5 ($[M+1]^+$, 100).

Characterization of 8f (Chloracetyl-Gly-Gly-NH-$C_{12}H_{25}$)

White solid. m.p. 212-213°C; ^{1}H NMR (300 MHz, d_6-DMSO) δ 0.86 (t, J = 6 Hz, 3H), 1.24 (br, 18H), 1.36-1.41 (m, 2H), 3.04 (q, J = 6.6 Hz, 2H), 3.66 (s, 2H), 3.78 (s, 2H), 4.14 (s, 2H), 7.69 (br, 1H), 8.18 (br, 1H), 8.46 (br, 1H); ^{13}C NMR (75 MHz, d_6-DMSO) δ 168.37, 168.13, 165.35, 42.55, 42.46, 42.02, 38.35, 31.38, 29.11, 28.82, 27.37, 26.55, 26.36, 22.15, 13.94; MALDI-TOF MS m/z Calcd for $C_{18}H_{34}ClN_3O_3$: 379.23. Found: 379.5 ($[M]^+$, 100).

Characterization of gelators 1-6

Characterization of 1 (MPTTF-CH_2CO-Gly-Phe-NH-$C_{12}H_{25}$)

Yellow solid. m.p. 124-125°C; ^{1}H NMR (300 MHz, d_6-DMSO) δ 0.83-0.90 (m, 9H), 1.24 (br, 18H), 1.29-1.33 (m, 2H), 1.35-1.45 (m, 4H), 1.50-1.59 (m, 4H), 2.72-2.83 (m, 2H), 2.85 (t, J = 6.9 Hz, 4H), 2.93-3.06 (m, 2H), 3.57-3.80 (m, 2H), 4.40-4.47 (m, 1H), 4.58 (s, 2H), 6.76 (s, 2H), 7.17-7.27 (m, 5H), 7.87 (t, J = 5.1 Hz, 1H), 8.17-8.22 (m, 2H); ^{13}C NMR (75 MHz, d_6-DMSO) δ 170.65, 168.44, 167.82, 138.00, 129.36, 128.30, 126.99, 126.50, 121.06, 120.98, 117.43, 114.96, 108.02, 54.36, 52.60, 42.31, 38.12, 35.30, 31.60, 29.39, 29.34, 29.16, 29.03, 26.62, 22.40, 21.17, 14.24, 13.68; MALDI-TOF MS m/z Calcd for $C_{41}H_{60}N_4O_3S_6$: 848.30. Found: 848.3 ($[M]^+$, 100); elemental analysis calcd for $C_{41}H_{60}N_4O_3S_6$: C 57.98, H 7.12, N 6.60; found: C 58.15, H 7.43, N 6.31.

Characterization of 2 (MPTTF-CH_2CO-Leu-Phe-NH-$C_{12}H_{25}$)

Yellow solid. m.p. 139-140°C;^{1}H NMR (300 MHz, d_6-DMSO) δ 0.83-0.90 (m, 15H), 1.24 (br, 19H), 1.35-1.45 (m, 6H), 1.50-1.59 (m, 6H), 2.63-2.80 (m, 2H), 2.85 (t, J = 6.9 Hz, 4H), 2.93-3.02 (m, 2H), 4.13-4.23 (m, 1H), 4.37-4.46 (m, 1H), 4.55 (s, 2H), 6.72 (s, 1H), 6.74 (s, 1H), 7.17-7.23 (m, 5H), 7.70 (t, J = 5.4 Hz, 1H), 8.02 (d, J = 8.1 Hz, 1H), 8.23 (d, J = 7.2 Hz, 1H); ^{13}C NMR (75

MHz, d_6-DMSO) δ 171.89, 170.69, 167.80, 138.82, 138.34, 129.67, 128.56, 127.28, 126.77, 117.66, 115.21, 108.26, 54.31, 52.24, 41.44, 38.09, 35.61, 31.91, 29.71, 29.66, 29.44, 29.40, 29.35, 27.05, 26.94, 24.59, 24.33, 23.44, 22.99, 22.71, 22.31, 21.42, 14.55, 13.99; MALDI-TOF MS m/z Calcd for $C_{45}H_{68}N_4O_3S_6$: 903.36. Found: 902.3 ([M-1]$^+$, 100); elemental analysis calcd for $C_{45}H_{68}N_4O_3S_6$: C 59.69, H 7.57, N 6.19; found: C 59.97, H 7.93, N 6.54.

Characterization of 3 (MPTTF-CH_2CO-Phe-Phe-NH-$C_{12}H_{25}$)

Yellow solid. m.p. 157-158^{o}C; ^{1}H NMR (300 MHz, d_6-DMSO) δ0.83-0.90 (m, 9H), 1.23 (br, 18H), 1.27-1.33 (m, 2H), 1.35-1.45 (m, 4H), 1.50-1.59 (m, 4H), 2.69-2.80 (m, 2H), 2.85 (t, J = 6.9 Hz, 4H), 2.91-3.07 (m, 4H), 4.41-4.54 (s, 4H), 6.60 (s, 2H), 7.13-7.27 (m, 10H), 7.79 (t, J = 5.4 Hz, 1H), 8.16 (d, J = 8.1 Hz, 1H), 8.26 (t, J = 8.1 Hz, 1H); ^{13}C NMR (75 MHz, d_6-DMSO) δ170.86, 167.27, 138.23, 137.86, 129.81, 129.72, 128.60, 128.54, 127.30, 126.80, 121.37, 117.66, 115.04, 108.42, 54.60, 54.40, 38.40, 38.20, 35.60, 31.89, 29.67, 29.62, 29.48, 29.36, 29.31, 26.89, 22.68, 21.47, 14.53, 13.97; MALDI- TOF MS m/z Calcd for $C_{48}H_{66}N_4O_3S_6$: 938.35. Found: 939.5 ([M+1]$^+$, 100); elemental analysis calcd for $C_{48}H_{66}N_4O_3S_6$: C 61.37, H 7.08, N 5.96; found: C 61.71, H 7.42, N 5.65.

Characterization of 4 (MPTTF-CH_2CO-Leu-Leu-NH-$C_{12}H_{25}$)

Yellow solid. m.p. 131-132^{o}C; ^{1}H NMR (300 MHz, d_6-DMSO) δ0.81-0.90 (m, 21H), 1.23 (br, 18H), 1.30-1.45 (m, 8H), 1.49-1.63 (m, 8H), 2.85 (t, J = 6.9 Hz, 4H), 2.92-3.07 (m, 2H), 4.18-4.28 (m, 2H), 4.58 (s, 2H), 6.76 (s, 2H), 7.68 (t, J = 5.4 Hz, 1H), 7.93 (d, J = 8.4 Hz, 1H), 8.26 (t, J = 7.8 Hz, 1H); ^{13}C NMR (75 MHz, d_6-DMSO) δ174.28, 171.99, 167.68, 127.13, 121.30, 117.69, 115.20, 108.33, 52.14, 51.58, 41.46, 35.59, 31.90, 29.66, 29.65, 29.64, 29.34, 29.32, 26.89, 26.78, 24.83, 24.74, 23.57, 23.46, 22.72, 22.68, 22.26, 21.47, 14.55, 13.97; MALDI-TOF MS m/z Calcd for $C_{42}H_{70}N_4O_3S_6$: 870.38. Found: 869.3 ([M-1]$^+$, 100); elemental analysis calcd for $C_{42}H_{70}N_4O_3S_6$: C 57.89, H 8.10, N 6.43; found: C 58.12, H 8.35, N 6.15.

Characterization of 5 (MPTTF-CH_2CO-Gly-Leu-NH-$C_{12}H_{25}$)

Yellow solid. m.p. 137-138^{o}C; ^{1}H NMR (300 MHz, d_6-DMSO) δ0.81-0.90 (m, 15H), 1.24 (br, 18H), 1.33-1.45 (m, 7H), 1.50-1.59(m, 6H), 2.85 (t, J = 6.9 Hz, 4H), 2.91-3.06 (m, 2H), 3.70-3.82 (m, 2H), 4.20-4.27 (m, 1H), 4.61 (s, 2H), 6.78 (s, 2H), 7.82 (t, J = 5.1 Hz, 1H), 8.02 (d, J = 8.1 Hz, 1H), 8.25 (t, J = 5.1 Hz, 1H); ^{13}C NMR (75 MHz, d_6-DMSO) δ 172.01, 168.74, 168.28, 127.29, 121.34, 117.71, 115.15, 108.37, 51.57, 42.73, 41.63, 35.59, 31.89, 29.63, 29.49, 29.32, 26.91, 26.87, 26.85, 24.72, 23.51, 22.69, 22.26, 22.22, 21.47, 14.52, 13.97; MALDI-TOF MS m/z Calcd for $C_{38}H_{62}N_4O_3S_6$: 814.31. Found: 813.5 ([M-1]$^+$, 100); elemental analysis calcd for

$C_{38}H_{62}N_4O_3S_6$: C 55.98, H 7.66, N 6.87; found: C 56.29, H 7.98, N 6.52.

Characterization of 6 (MPTTF-CH_2CO-Gly-Gly-NH-$C_{12}H_{25}$)

Yellow solid. m.p. 144-145°C; ^{1}H NMR (300 MHz, d_6-DMSO) δ0.83-0.90 (m, 9H), 1.24 (br, 18H), 1.33-1.45 (m, 6H), 1.50-1.59 (m, 4H), 2.85 (t, J = 6.9 Hz, 4H), 3.00 (q, J = 6.3 Hz, 2H), 3.65 (d, J = 5.7 Hz, 2H), 3.74 (d, J = 5.4 Hz, 2H), 4.62 (s, 2H), 6.79 (s, 2H), 7.61 (t, J = 5.1 Hz, 1H), 8.20 (t, J = 5.7 Hz, 1H), 8.36 (t, J = 5.1 Hz, 1H); ^{13}C NMR (75 MHz, d_6-DMSO) δ 169.34, 168.88, 168.63, 127.23, 121.29, 117.60, 115.32, 108.18, 52.90, 43.02, 42.57, 35.59, 31.90, 29.70, 29.66, 29.58, 29.39, 29.34, 27.02, 22.70, 21.47, 14.54, 13.98; MALDI-TOF MS m/z Calcd for $C_{34}H_{54}N_4O_3S_6$: 758.25. Found: 757.3 ([M-1]$^+$, 100); elemental analysis calcd for $C_{34}H_{54}N_4O_3S_6$: C 53.79, H 7.17, N 7.38; found: C 54.05, H 7.41, N 7.03.

3. The gelation properties.

Table S1 Gelation tests for **1-6**.

Solvent	1	2	3	4	5	6
Methylcyclohexane	6.5[a](TG[b])	15.8(TG)	8.3(TG)	S	8.7(TG)	8.9(TG)
Cyclohexane	5.1(TG)	13.8(TG)	6.6(TG)	S	6.6(TG)	7.2(TG)
n-Hexane	IS	IS	IS	IS	IS	IS
Benzene	S	S	7.2(TG)	S	S	5.7(TG)
Toluene	S	S	5.8(TG)	S	S	4.8(TG)
Chlorobenzene	S	S	11.5(TG)	S	S	3.6(TG)
Xylene	S	S	6.4(TG)	S	S	4.1(TG)
Nitrobenzene	S	S	S	S	S	6.0(TG)
CH_2Cl_2	S	S	S	S	S	S
$CHCl_3$	S	S	S	S	S	S
CCl_4	S	S	S	S	S	S
CH_3CN	P	P	P	P	P	3.2(OG)
EA	PG	S	P	S	S	1.8(OG)
THF	S	S	S	S	S	S
Methanol	P	13.8(OG)	P	P	S	P
Ethanol	S	13.8(OG)	P	S	S	4.8(OG)
Acetone	P	S	P	S	S	29(OG)
Diethyl ether	IS	sS	IS	S	PG	IS
DMF	S	S	S	S	S	S
DMSO	S	S	S	S	S	S
Kerosene	sS	2.4(OG)	1.7(OG)	16(OG)	2.2(OG)	IS

[a]OG = opaque gel; TG = transparent gel; PG = part gel; P = precipitation;
S = soluble; IS = insoluble; sS = slight soluble.
[b]CGC = the critical gelation concentrations (mg/mL) at room temperature.

4. Gelation abilities in other solvents

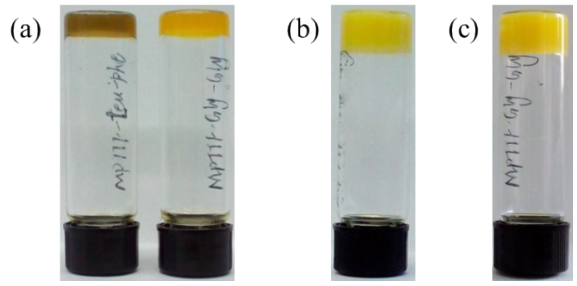

Figure S1. The photographs of gelators (a) **2** and **6** in ethanol, (b) **6** in acetonitrile and (c) **6** in ethyl acetate.

5. FE-SEM images

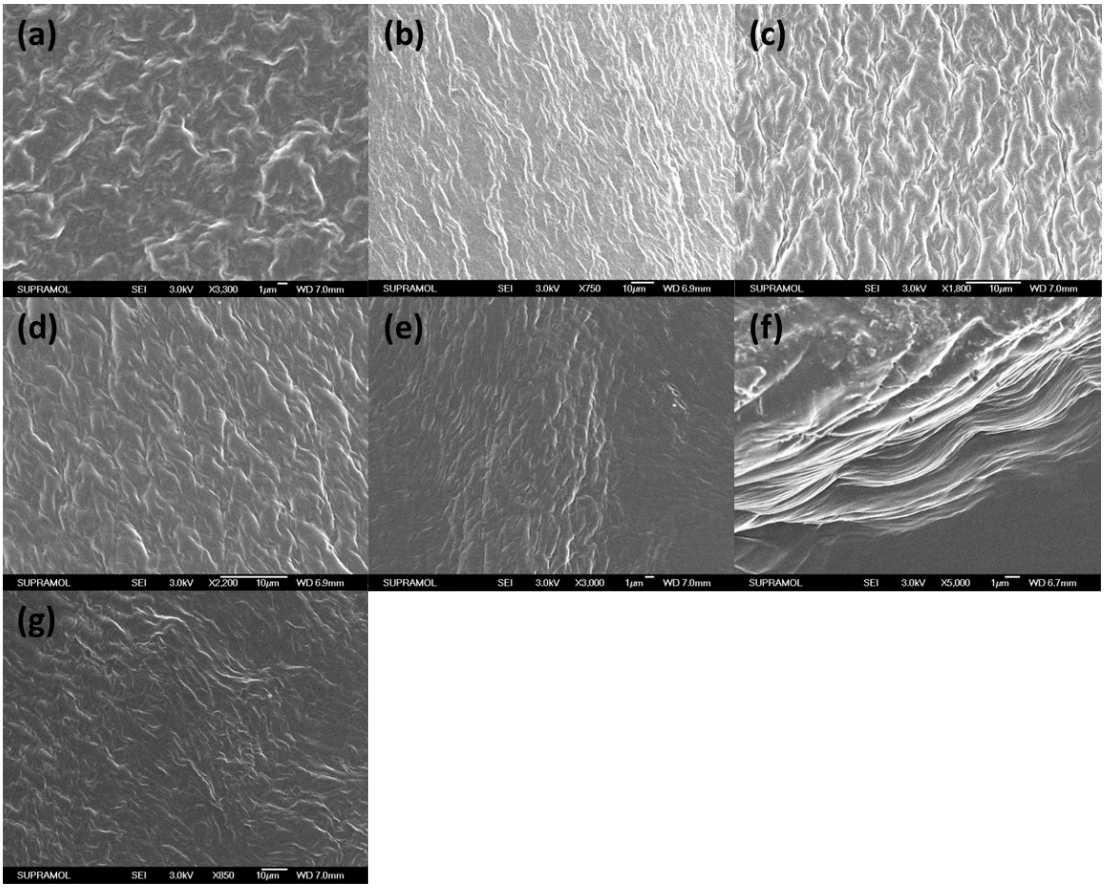

Figure S2. FE-SEM images of **1**, **2**, **3**, **5** and **6** xerogels obtained from cyclohexane (a-e) and **5** and **6** xerogels from toluene (f-g).

6. WAXRD studies

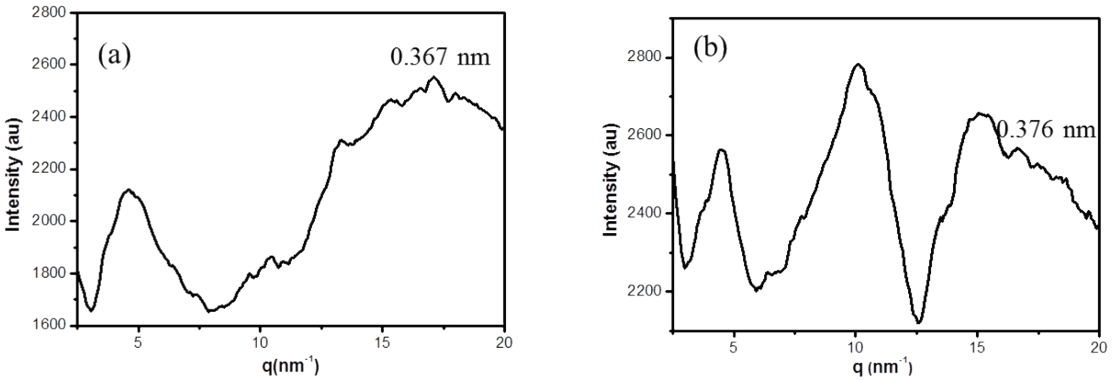

Figure S3. WAXRD patterns of xerogels of **3** (-Phe-Phe-) from cyclohexane (a) and toluene (b).

7. Data from FT-IR and UV-Vis

Table S2 Summary data of FT-IR and UV-Vis spectra of **3** (-Phe-Phe-) in DMSO solution and xerogel from cyclohexane and toluene, respectively.

	νN–H (cm^{-1})	νC=O (cm^{-1})	δN–H (cm^{-1})	UV-Vis (nm)
DMSO solution	3411, 3281	1664	1550	291, 325, 455
xerogel from toluene	3275	1638	1553	296, 329, 480
xerogel from cyclohexane	3275	1638	1554	296, 328, 481

8. Anions responsive

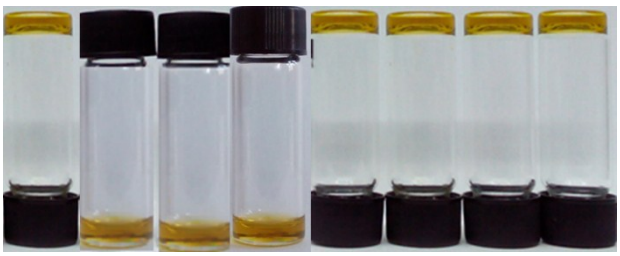

Figure S4. Photographs of the **3** (-Phe-Phe-) gel (toluene, 6 mg/mL) upon the addition of 3.0 equiv. of each anion. From left to right： native gel, + F^-, Cl^-, $H_2PO_4^-$, Br^-, I^-, HSO_4^-, AcO^-.

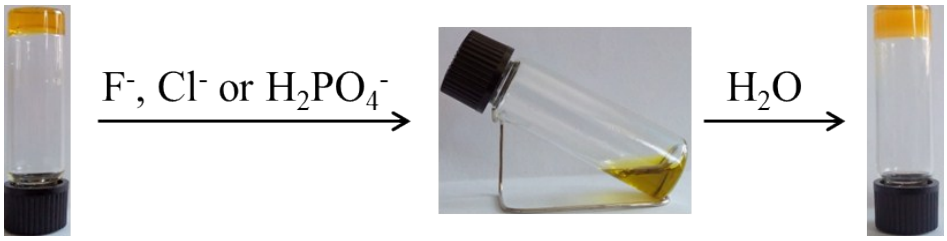

Figure S5. Reversible sol–gel phase transition of the **3** (-Phe-Phe-) gel in cyclohexane trigged by anions and water.

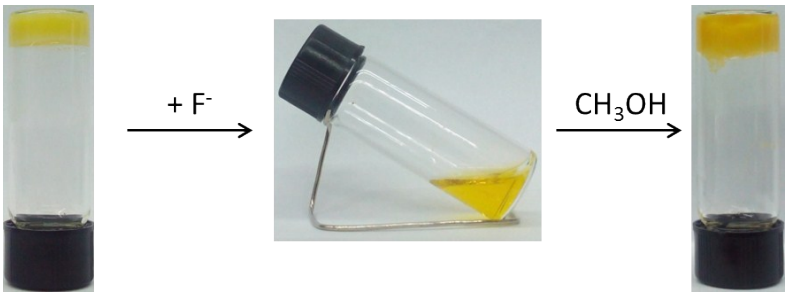

Figure S6. Reversible sol–gel phase transition of the **6** (-Gly-Gly-) gel in CH_3CN trigged by anions and methanol.

9. UV-Vis spectra changes by addition of anions

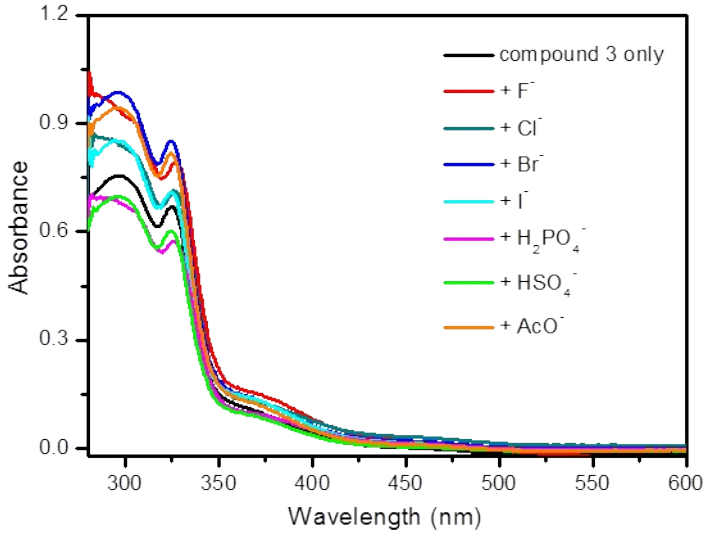

Figure S7. UV-Vis spectra of **3** (-Phe-Phe-) in DMSO (5×10^{-5} M) with addition of 3.0 equiv. different anions, respectively.

10. CV curves

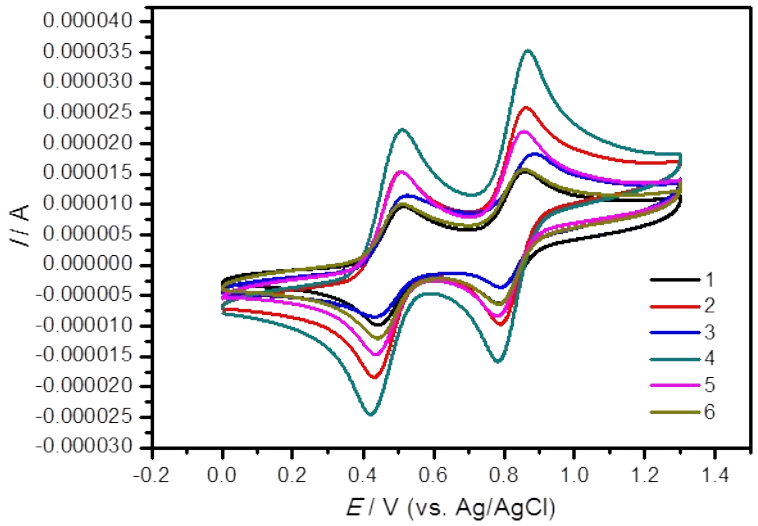

Figure S8. Cyclic voltammograms of **1-6** (1×10^{-3}M) in CH_2Cl_2-CH_3CN (1 : 1, v/v) containing 0.1 M Bu_4NPF_6. Scan rate was 100 mV s^{-1}.

11. The CT intensity

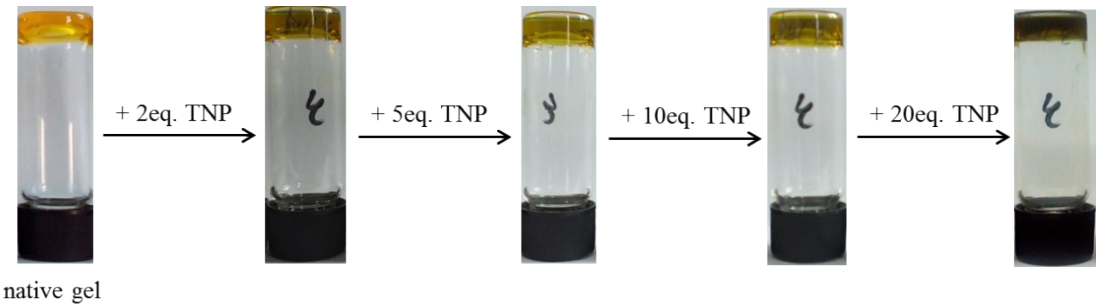

Figure S9. The color changes of the CT complex gels of **3** (-Phe-Phe-) with increasing of TNP concentration in toluene.

12. T_{gel} of CT complex gels

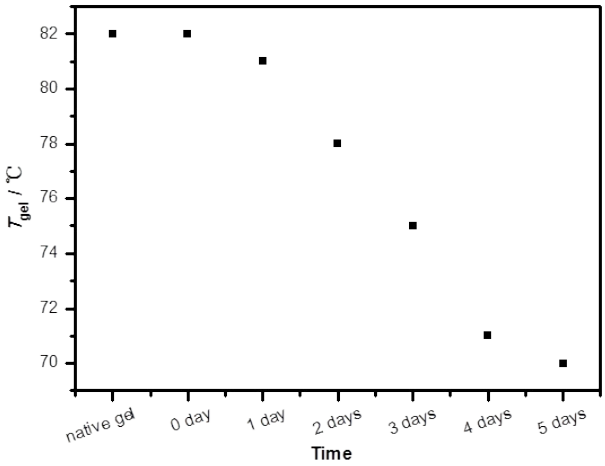

Figure S10. The T_{gel} of the CT complex gel (10 mg/mL) of **3** (-Phe-Phe-) in different period after addition in 2.0 eq. TNP in toluene.

13. The CV curves of CT complex gels

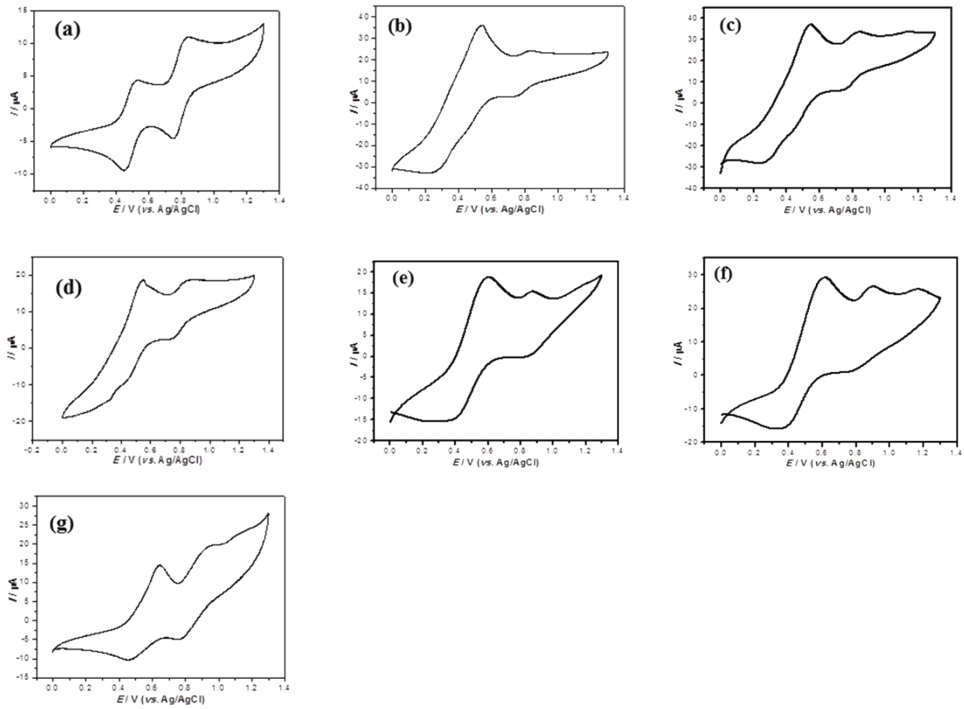

Figure S11. The CV curves of the CT complex xerogels in different period after addition of 2.0 eq. TNP from toluene: (a) native xerogel of **3** (-Phe-Phe-), incubated with TNP (b) 0 day, (c) 1 day, (d) 2 days, (e) 3 days, (f) 4 days and (g) 5 days.

14. The data from CV curves of CT complex gels

Table S3 The oxidation potentials of xerogels of TTF unit when incubated with 2.0 equiv. TNP in different times from toluene.

Potential	Native gel	+ TNP 0 day	+ TNP 1 day	+ TNP 2 days	+ TNP 3 days	+ TNP 4 days	+ TNP 5 days
E_{ox}^{1} (V)	0.522	0.543	0.545	0.550	0.601	0.615	0.644
E_{ox}^{2} (V)	0.833	0.831	0.838	0.850	0.871	0.898	0.946

15. Interaction with TNP on TLC strips

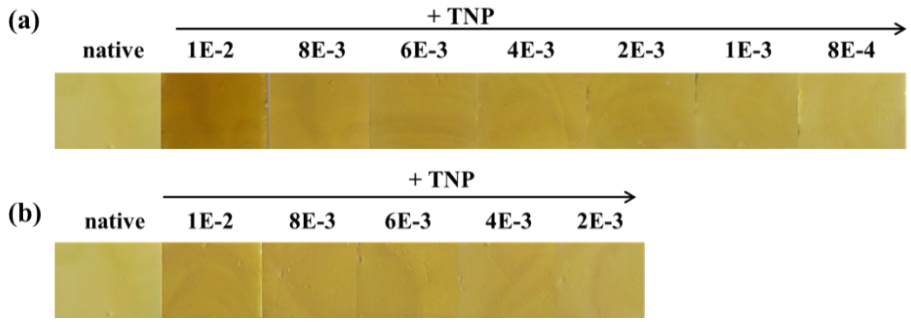

Figure S12. Photographs of **3**-coated TLC strips after dipping into solutions of TNP in toluene (a) and water (b).

16. The reversible color changes of chemical redox

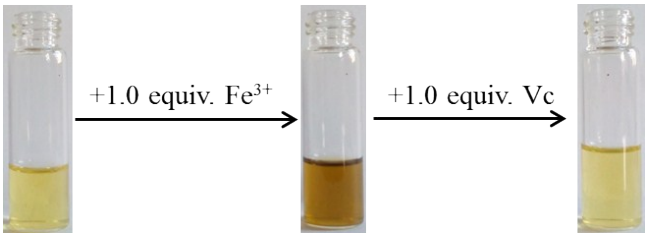

Figure S13. The color changes of **3** (-Phe-Phe-) in ethanol (1×10^{-4} M) solution by chemical redox.

17. Absorption of dyes by toluene gel

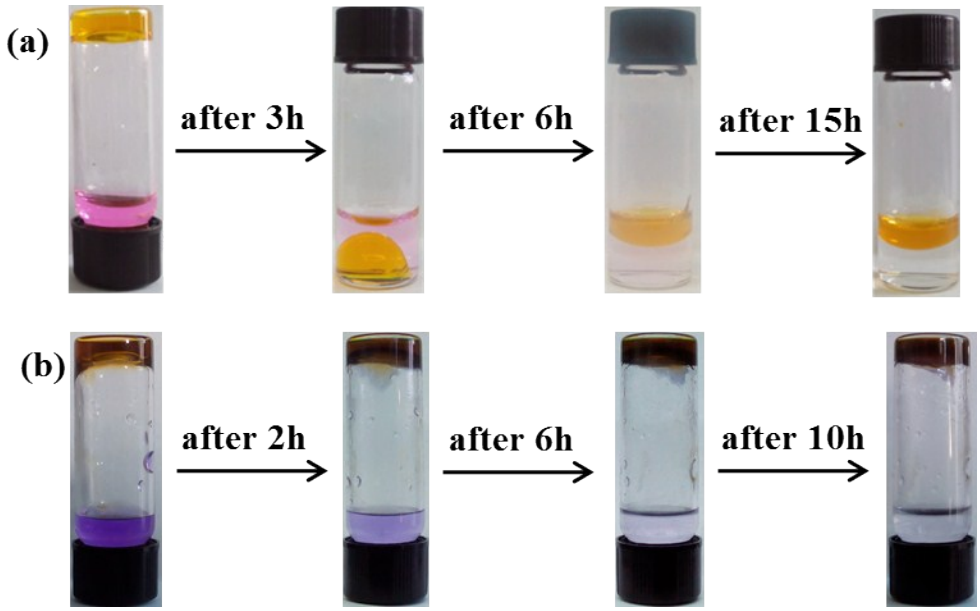

Figure S14. Photographs of an aqueous solution of Rhodamine B (a) and Crystal Violet (b) after adsorption by organogel **3** in toluene in different times; 1.0 mL of Crystal Violet or Rhodamine B (2×10^{-5} M) was added on the top of 0.4 mL gel and the samples were tested at room temperature.

18. Structures of the dye molecules

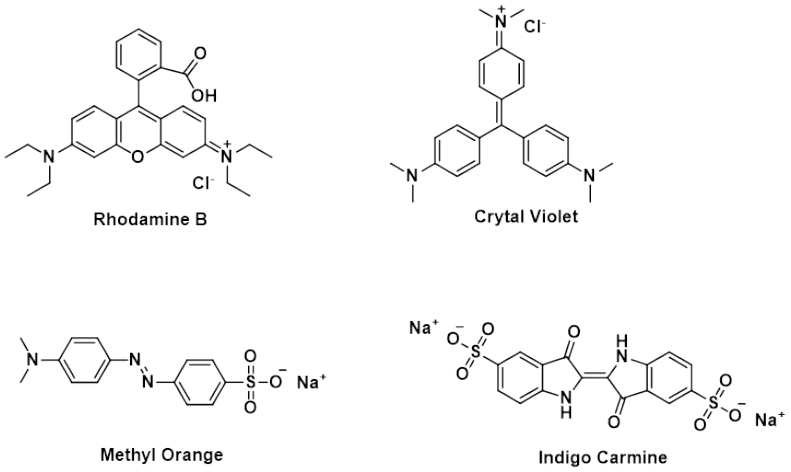

Scheme S1. The structures of the dye molecules.

19. Absorption spectra of Methyl Orange and Indigo Carmine

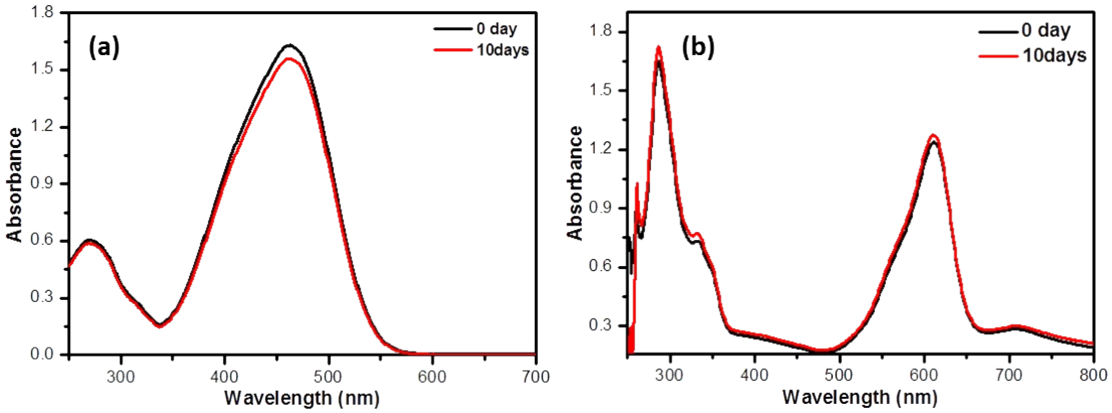

Figure S15. The absorption spectra of aqueous solution of Methyl Orange (a) and Indigo Carmine (b) by absorption of cyclohexane gel of **3** in different times.